Nanoscale

Cite this: *Nanoscale*, 2011, **3**, 1477

www.rsc.org/nanoscale

COMMUNICATION

A simple and scalable graphene patterning method and its application in CdSe nanobelt/graphene Schottky junction solar cells

Yu Ye,[a] Lin Gan,[b] Lun Dai,*[a] Yu Dai,[a] Xuefeng Guo,[b] Hu Meng,[a] Bin Yu,[a] Zujin Shi,[b] Kuanping Shang[a] and Guogang Qin*[a]

Received 17th December 2010, Accepted 28th January 2011
DOI: 10.1039/c0nr00999g

We have developed a simple and scalable graphene patterning method using electron-beam or ultraviolet lithography followed by a lift-off process. This method, with the merits of: high pattern resolution and high alignment accuracy, being free from additional etching or harsh processes, being universal to arbitrary substrates, and being compatible to Si microelectronic technology, can easily be applied to diverse graphene-based devices, especially in array-based applications, where large-scale graphene patterns are desired. We have applied this method to fabricate CdSe nanobelt (NB)/graphene Schottky junction solar cells, which have potential applications in integrated nano-optoelectronic systems. A typical as-fabricated solar cell shows excellent photovoltaic behavior, with an open-circuit voltage of ~0.51 V, a short-circuit current density of ~5.75 mA cm^{-2}, and an energy conversion efficiency of ~1.25%. We attribute the high performance of the cell to the as-patterned high-performance graphene, which can form an ideal Schottky contact with CdSe NB. Our results suggest that both the developed graphene patterning method and the as-fabricated CdSe NB/graphene Schottky junction solar cells have reachable application prospects.

Introduction

Graphene, a new class of two-dimensional, conjugated, honeycomb lattice structured carbon material, has drawn widespread attention owing to its fascinating physical properties, such as quantum electronic transport,[1,2] high electrical conductivity,[3] ultrahigh mobility,[4] high elasticity,[5] and high transparency.[6] The recent advances in the large-scale synthesis of graphene by chemical vapor deposition (CVD) on Ni[7,8] and Cu[9,10] films open up various macroscopic applications of graphene, including light-emitting diodes,[11] solar cells,[12] transistors,[13] and nanogenerators.[14] However, key technical challenges remain in several areas, such as improving film uniformity, scaling-up to large-area patterning techniques for array-based applications *etc.*[10,15] So far, a variety of techniques have been reported in an effort to solve the latter problem, including spatially selective CVD,[16] transfer printing using polydimethylsiloxane (PDMS) or transfer stamping using highly oriented pyrolytic graphite (HOPG) stamps,[17,18] conventional photolithography followed by O_2 reactive ion etching (RIE),[19] and helium ion ablation.[20] These methods suffer from a variety of limitations, such as insufficient resolution,[16] high cost,[17,18] complex or inconvenient processing steps,[20] and/or process-induced damage of electronic properties.[19]

In this communication, we report a simple and scalable graphene patterning method using electron-beam lithography (EBL) or ultraviolet (UV) lithography followed by a lift-off process. This method has the merits of: high pattern resolution and high alignment accuracy, being free from additional etching or harsh processes, being universal to arbitrary substrates, and being compatible to Si microelectronic technology, and can easily be applied to diverse graphene-based devices, especially in array-based applications, where fabricating and aligning large-scale graphene patterns with high resolution and high alignment accuracy are desired.

CdSe, due to its suitable bandgap (1.74 eV) for solar light absorption, is an important photovoltaic (PV) material, and has attracted more and more attention recently.[21,22] Graphene has good transparency and conductivity, and can, in principle, form a good Schottky contact with CdSe. We have utilized the developed graphene patterning method to fabricate CdSe nanobelt (NB)/graphene Schottky junction solar cells.[23] Under air mass (AM) 1.5 global (1.5 G) illumination with a calibrated solar simulator, such a Schottky junction solar cell exhibits an open-circuit voltage (V_{OC}) of ~0.51 V, a short-circuit current density (J_{SC}) of ~5.75 mA cm^{-2}, and a fill factor (*FF*) of ~42.7%, with an energy conversion efficiency (η) of ~1.25%. These CdSe NB/graphene Schottky junction solar cells are promising candidates for novel third generation solar cells, which have potential applications in integrated nano-optoelectronic systems.

Experimental section

Both the *n*-CdSe NBs[24] and the graphene[25] used in this work were synthesized *via* the CVD method. For synthesis of large-scale uniform monolayer graphene, a quartz boat loaded with the Cu foils was placed in a furnace, then the system was evacuated and heated to 1000 °C under a 10 cm^3 min^{-1} flow of H_2 at a pressure of about 50 Pa. After stabilizing the Cu foils at the desired temperature, CH_4 with

[a]*State Key Lab for Mesoscopic Physics and School of Physics, Peking University, Beijing, 100871, China. E-mail: lundai@pku.edu.cn; qingg@pku.edu.cn*
[b]*College of Chemistry and Molecular Engineering, Peking University, Beijing, 100871, China*

a flow-rate of 1.1 cm^3 min^{-1} was introduced at a pressure of about 60 Pa for 15 min. After the growth, the substrates were cooled down to room temperature.

The as-synthesized graphenes were transferred by the stamp method with the help of PMMA[7] to Si/SiO_2 (300 nm) substrates for Raman and electrical property characterization, and to quartz substrates for transparency characterization. The Raman measurements were performed with a microzone confocal Raman spectroscope (Renishaw inVia microRaman system) equipped with a color charge-coupled device (CCD). The excitation wavelength was 514 nm. The electrical property was measured by a Hall measurement system (Accent HL5500). The transparency was measured by a UV-vis-NIR recording spectrophotometer (Shimadzu UV-3100). The room-temperature electrical transport and PV properties of the CdSe NB/graphene Schottky junction solar cells were characterized with a semiconductor characterization system (Keithley 4200) and a solar simulator (Newport 91160-1000) with a calibrated illumination power density of 100 mW cm^{-2}.

Fig. 1 shows a schematic illustration of the simple and scalable graphene patterning processes. First, large-scale graphene was synthesized on a Cu foil by the CVD method (Fig. 1a). After a layer of PMMA (200 nm) was spun on the graphene (Fig. 1b), the underlying Cu foil was etched using 1 M $FeCl_3$ solution (Fig. 1c) for 1–2 h. The graphene/PMMA film floating in the etchant was then collected manually and placed into deionized (DI) water. The device substrate (the Si/SiO_2 substrate in our case) was prepared as follows: first, a layer of PMMA (200 nm) was spun on it (Fig. 1d). Then, EBL (FEI Strata DB 235) was employed to pattern the PMMA into the desired shapes, with high resolution, at the desired locations, with high alignment accuracy (Fig. 1e). After that, the graphene/PMMA film floating on the DI water was manually collected onto the patterned device substrate (Fig. 1f). The flexibility of the graphene/PMMA film lets it conform into the windows area and contact with the bare devices substrate. There exists a strong adhesive interaction between graphene and SiO_2.[26] This adhesion can be further enhanced by a heat treatment.[27] Lastly, all of the PMMA was dissolved in acetone (Fig. 1g). During this process, the buoyancy force will drive the graphenes atop the PMMA to separate from those adhered to the SiO_2 and float up to the surface of the liquid. This process is similar to a lift-off process. It is worth noting that UV lithography, which has the advantage of manufacturing large-area graphene patterns on basically arbitrary substrates, can also be used to replace EBL in this method (as demonstrated below).

Fig. 4a shows a schematic illustration of the CdSe NB/graphene Schottky junction solar cell. One In/Au (10/100 nm) ohmic electrode was prepared at one end of the CdSe NB by UV lithography, thermal evaporation, and lift-off processes. The graphene film was made on the other end of the NB with the developed graphene patterning method using UV lithography.

Results and discussion

Fig. 2a–e show field-emission scanning electron microscope (FESEM) images of the patterned graphene fabricated by EBL, with the shapes of micro-scale squares, triangles, letter As, nano-scale cirques and lines, respectively, on SiO_2/Si substrates. The edges of these patterns are sharply demarcated from the substrates. Here, the minimum linewidth is ~350 nm. It is worth noting that the heat treatment (90 °C, 30 min in our case) is needed before the lift-off process. Moreover, the thinner the PMMA, the smaller the structure size of graphene that can be obtained. The right panel of Fig. 2f shows an optical image of a patterned graphene fabricated with UV lithography (the photoresist thickness is about 1.0 μm) on a flexible transparent substrate. We can see that the macro-scale graphene pattern faithfully copies the feature on the photomask (the left panel).

Before utilizing this graphene patterning method to fabricate CdSe NB/graphene Schottky junction solar cells, the synthesized

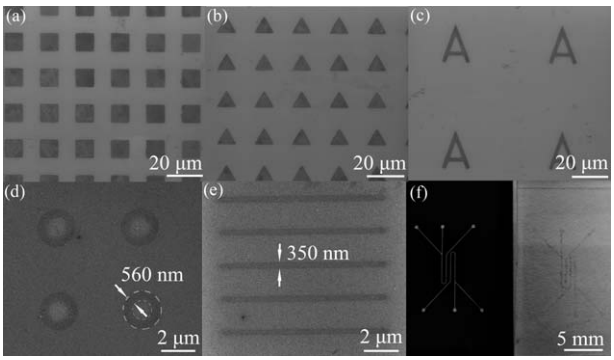

Fig. 2 (a)–(e) FESEM images of the patterned graphene by EBL with shapes of micro-scale squares, triangles, letter As, nano-scale cirques and lines, respectively, on SiO_2/Si substrates. (f) Left panel: optical image of the photomask. Right panel: optical image of the patterned graphene by UV lithography on a flexible transparent substrate.

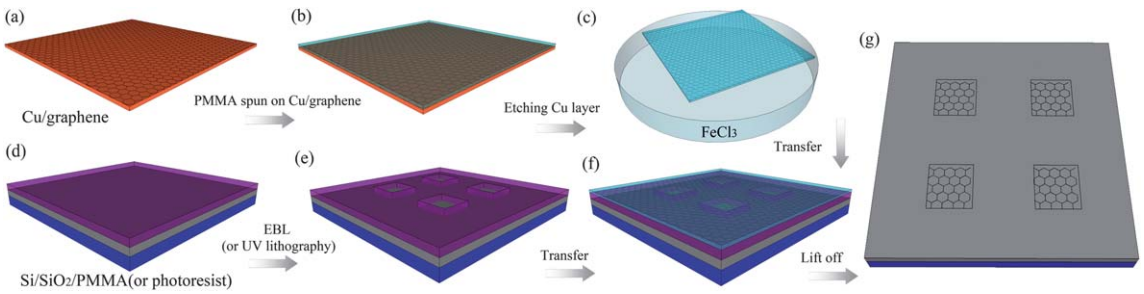

Fig. 1 A schematic illustration of the simple and scalable graphene patterning processes. (a) Synthesizing a large-scale graphene film on a Cu foil. (b) A layer of PMMA was spun on the Cu foil with the synthesized graphene on the top. (c) The underlying Cu film was etched using 1M $FeCl_3$ solution. (d) A layer of PMMA (or photoresist) was spun on a device substrate. (e) EBL (or UV lithography) was employed to pattern the PMMA (or photoresist) into desired shapes at desired locations. (f) The graphene/PMMA film was manually collected onto the patterned device substrate. (g) PMMA (or photoresist) together with the graphene atop it was removed by a lift-off process in acetone, and the patterned graphene was formed on the device substrate.

graphenes were characterized. Fig. 3a shows a typical Raman spectrum of the graphenes. It shows two main peaks: a narrow linewidth (~27 cm^{-1}) G-band peak (~1594 cm^{-1}) and a narrow linewidth (~45 cm^{-1}) 2D-band peak (~2689 cm^{-1}). Their intensity ratio ($I_{2D} : I_G$) is about 2.4, indicating the formation of monolayer graphene.[7] In addition, the defect-related[28] D-band peak (~1358 cm^{-1}) is weak, indicating the high quality of the graphene. Fig. 3b shows the transparency spectrum of the graphene. It can be seen that high transparency (>98%) occurs in the wavelength range longer than 500 nm. The typical sheet resistance of the graphenes is about 345 Ω $\square^{-1}$.

An FESEM image of an as-fabricated CdSe NB/graphene Schottky junction solar cell is shown in Fig. 4b. The Au (100 nm) electrode, which can form an ohmic contact with the graphene, was used later on for welding purposes.

The mechanism of Schottky junction solar cells can be qualitatively understood by plotting the energy band diagram. Fig. 5a shows the energy diagram of a CdSe NB/graphene Schottky junction solar cell under illumination. Due to the work function difference between the graphene ($\Phi_G \sim 4.66$ eV)[29] and CdSe ($\Phi_{CdSe} \sim 4.2$ eV),[30] a built-in potential (V_i) forms in the CdSe near the CdSe NB/graphene interface. Under illumination, the photogenerated holes (h^+) and electrons (e^-) are driven toward the Schottky electrode (graphene film) and CdSe NB, respectively, by the built-in electric field. When the solar cell is open-circuited, the separated photogenerated electrons and holes will produce an open-circuit voltage V_{OC}. When the solar cell is short-circuited, the extracted photogenerated carriers will transit through the external circuit, generating a short-circuited current I_{SC}.

Fig. 5b shows the room-temperature *I–V* characteristic (in the dark) of the solar cell depicted in Fig. 4b on a semi-log scale. We can see that the *I–V* curve shows an excellent rectification characteristic.

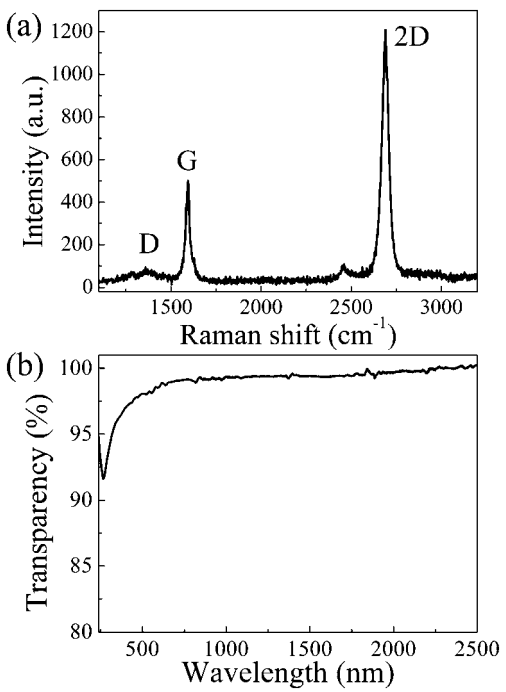

Fig. 3 (a) A Raman spectrum of the graphene on a Si/SiO_2 substrate. (b) A transparency spectrum of the graphene on a quartz substrate.

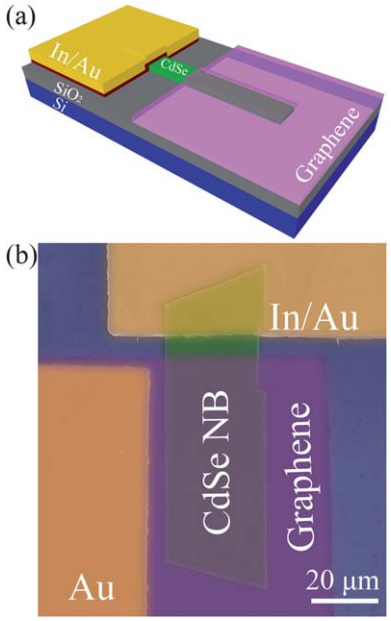

Fig. 4 (a) A schematic illustration of the CdSe NB/graphene Schottky junction solar cell. (b) An FESEM image of a CdSe NB/graphene Schottky junction solar cell.

An on/off current ratio of ~7.5×10^4 can be obtained when the voltage changes from +1 to −1 V. For Schottky junction diodes made on high-mobility semiconductors, such as Si and CdSe *etc.*, the current *I* is determined by the thermionic emission of electrons and can be described by the equation $I = I_0[\exp(eV/nkT) - 1]$,[31] where I_0 is the reverse saturation current, *e* is the electronic charge, *V* is the applied bias, *n* is the diode ideality factor, *k* is the Boltzmann constant, and *T* is the absolute temperature. By fitting the measured *I–V* curve with the above equation, we obtain $n = 1.17$. Here, *n* is quite close to the value of an ideal Schottky junction ($n = 1$).[32] All of these results indicate that the graphene film has formed a good Schottky contact with the CdSe NB.

Fig. 5c shows the room-temperature *I–V* characteristic of the solar cell depicted in Fig. 4b under AM 1.5 G illumination. We can see that this cell exhibits an excellent PV behavior with an open-circuit voltage (V_{OC}) of about 0.51 V, a short-circuit current density (J_{SC}) of about 5.75 mA cm^{-2}, and a fill factor (*FF*) of about 42.7%. The current density is calculated based on the effective Schottky junction area (the overlapping area of CdSe NB and graphene: ~1988.6 μm^2), where the charge separation takes place.[30] Therefore, we can estimate the corresponding energy conversion efficiency ($\eta = FF \cdot J_{SC} \cdot V_{OC}/P_{in}$, P_{in}: illumination light power density, 100 mW cm^{-2}) to be about 1.25%. We attribute the high performance of the CdSe NB/graphene Schottky solar cell to the high-performance graphene Schottky electrode fabricated with the developed graphene pattering method. It is worth noting that we have also fabricated CdSe NB/graphene Schottky junction solar cells with the most common graphene patterning method of UV lithography followed by the O_2 RIE process (not shown here).[19] Typical energy conversion efficiency for them is about 0.81%. We think that the RIE process may induce certain damage to graphene and/or the CdSe NB, which will further account for the noticeable decline in the device performance.

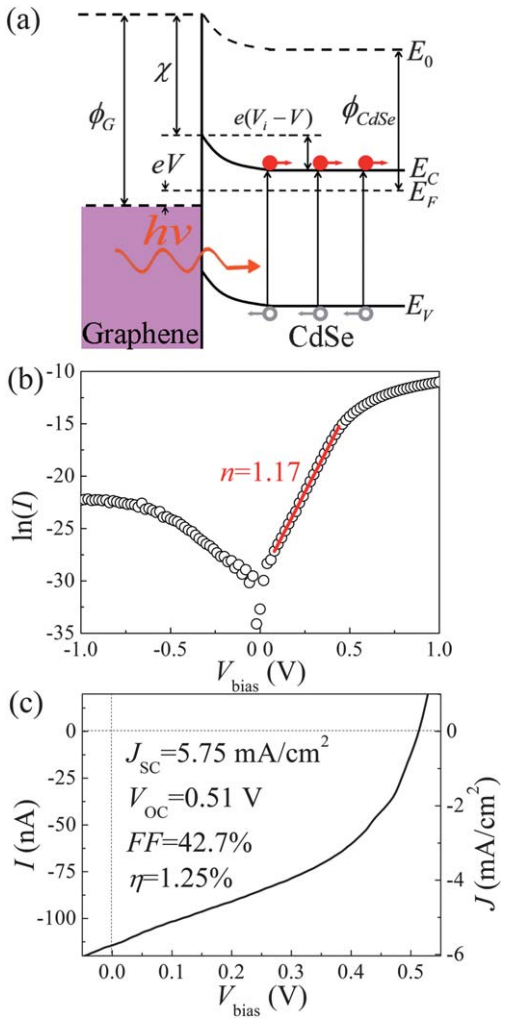

Fig. 5 (a) An energy diagram of a CdSe NB/graphene Schottky junction solar cell under illumination. Φ_G, Φ_{CdSe} are the work functions of graphene and CdSe, respectively. V_i is the built-in potential. V is the output voltage of the solar cell. χ is the electron affinity of CdSe. E_C, E_V and E_F correspond to the conduction band edge, valence band edge, and Fermi level of CdSe, respectively. E_0 corresponds to the vacuum level. (b) The room-temperature I–V characteristic (in dark) of the CdSe NB/graphene Schottky junction solar cell depicted in Fig. 4b on a semi-log scale. The red straight line shows the fitting result of the I–V curve by the equation $\ln(I) = eV/nkT + \ln(I_0)$. (c) The room-temperature I–V characteristic of the same solar cell under the AM 1.5 G illumination with light intensity of 100 mW cm^{-2}.

Conclusion

In summary, we have developed a simple and scalable graphene patterning method using electron-beam or UV lithography followed by a lift-off process. This method will accelerate the application of graphene in diverse optoelectronic and electronic devices, especially in large-scale graphene array-based applications. Novel CdSe NB/graphene Schottky junction solar cells were fabricated using this developed graphene patterning method. Typical as-fabricated solar cells show excellent PV behavior with an AM 1.5 G energy conversion efficiency of up to 1.25%. These high-performance CdSe NB/graphene Schottky junction solar cells are promising candidates for novel third generation solar cells, which have potential applications in integrated nano-optoelectronic systems.

Acknowledgements

This work was supported by the National Natural Science Foundation of China (Nos. 10774007, 11074006, 10874011, 50732001), the National Basic Research Program of China (Nos.2006CB921607, 2007CB613402), and the Fundamental Research Funds for the Central Universities.

References

1 K. S. Novoselov, A. K. Geim, S. V. Morozov, D. Jiang, M. I. Katsnelson, I. V. Grigorieva, S. V. Dubonos and A. A. Firsov, *Nature*, 2005, **438**, 197–200.
2 D. A. Abanin and L. S. Levitov, *Science*, 2007, **317**, 641–643.
3 Z. S. Wu, W. C. Ren, L. B. Gao, J. P. Zhao, Z. P. Chen, B. L. Liu, D. M. Tang, B. Yu, C. B. Jiang and H. M. Cheng, *ACS Nano*, 2009, **3**, 411–417.
4 K. I. Bolotin, K. J. Sikes, Z. Jiang, M. Klima, G. Fudenberg, J. Hone, P. Kim and H. L. Stormer, *Solid State Commun.*, 2008, **146**, 351–355.
5 C. G. Lee, X. D. Wei, J. W. Kysar and J. Hone, *Science*, 2008, **321**, 385–388.
6 X. S. Li, Y. W. Zhu, W. W. Cai, M. Borysiak, B. Y. Han, D. Chen, R. D. Piner, L. Colombo and R. S. Ruoff, *Nano Lett.*, 2009, **9**, 4359–4363.
7 A. Reina, X. T. Jia, J. Ho, D. Nezich, H. Son, V. Bulovic, M. S. Dresselhaus and J. Kong, *Nano Lett.*, 2009, **9**, 30–35.
8 K. S. Kim, Y. Zhao, H. Jang, S. Y. Lee, J. M. Kim, K. S. Kim, J. H. Ahn, P. Kim, J. Y. Choi and B. Hong, *Nature*, 2009, **457**, 706–710.
9 X. S. Li, W. W. Cai, J. B. An, S. Kim, J. Nah, D. X. Yang, R. Piner, A. Velamakanni, I. Jung, E. Tutuc, S. K. Banerjee, L. Colombo and R. S. Ruoff, *Science*, 2009, **324**, 1312–1314.
10 S. Bae, H. Kim, Y. Lee, X. F. Xu, J. S. Park, Y. Zheng, J. Balakrishnan, T. Lei, H. R. Kim, Y. I. Song, Y. J. Kim, K. S. Kim, B. Ozyilmaz, J. H. Ahn, B. H. Hong and S. Iijima, *Nat. Nanotechnol.*, 2010, **5**, 574–578.
11 J. B. Wu, M. Agrawal, H. A. Becerril, Z. N. Bao, Z. F. Liu, Y. S. Chen and P. Peumans, *ACS Nano*, 2010, **4**, 43–48.
12 X. Wang, L. J. Zhi and K. Mullen, *Nano Lett.*, 2008, **8**, 323–327.
13 W. Liu, B. L. Jackson, J. Zhu, C. Q. Miao, C. H. Chung, Y. J. Park, K. Sun, J. Woo and Y. H. Xie, *ACS Nano*, 2010, **4**, 3927–3932.
14 D. Choi, M. Y. Choi, W. M. Choi, H. J. Shin, H. K. Park, J. S. Seo, J. Park, S. M. Yoon, S. J. Chae, Y. H. Lee, S. W. Kim, J. Y. Choi, S. Y. Lee and J. M. Kim, *Adv. Mater.*, 2010, **22**, 2187–2192.
15 L. H. Liu, G. Zorn, D. G. Castner, R. Solanki, M. M. Lerner and M. Yan, *J. Mater. Chem.*, 2010, **20**, 5041–5046.
16 H. Ago, I. Tanaka, C. M. Orofeo, M. Tsuji and K. I. Ikeda, *Small*, 2010, **6**, 1226–1233.
17 M. J. Allen, V. C. Tung, L. Gomez, Z. Xu, L. M. Chen, K. S. Nelson, C. W. Zhou, R. B. Kaner and Y. Yang, *Adv. Mater.*, 2009, **21**, 2098–2102.
18 D. S. Li, W. Windl and N. P. Padture, *Adv. Mater.*, 2009, **21**, 1243–1246.
19 W. Liu, L. J. Jackson, J. Zhu, C. Q. Miao, C. H. Chung, Y. J. Park, K. Sun, J. Woo and Y. H. Xie, *ACS Nano*, 2010, **4**, 3927–3932.
20 M. C. Lemme, D. C. Bell, J. R. Williams, L. A. Stern, B. W. H. Baugher, P. Jarillo-Herrero and C. M. Marcus, *ACS Nano*, 2009, **3**, 2674–2676.
21 Y. H. Yu, P. V. Kamat and M. Kuno, *Adv. Funct. Mater.*, 2010, **20**, 1464–1472.
22 S. Dayal, N. Kopidakis, D. C. Olson, D. S. Ginley and G. Rumbles, *Nano Lett.*, 2010, **10**, 239–242.
23 T. Dufaux, J. Boettcher, M. Burghard and K. Kern, *Small*, 2010, **6**, 1868–1872.
24 C. Liu, P. C. Wu, T. Sun, L. Dai, Y. Ye, R. M. Ma and G. G. Qin, *J. Phys. Chem. C*, 2009, **113**, 14478–14481.
25 L. Gan, S. Liu, D. N. Li, H. Gu, Y. Cao, Q. Shen, Z. X. Wang, Q. Wang and X. F. Guo, *Acta Phys. -Chim. Sin.*, 2010, **26**, 1151–1156.

26 D. S. Li, W. Windl and N. P. Padture, *Adv. Mater.*, 2009, **21**, 1243–1246.
27 S. P. Pan, J. M. Enlert, H. N. Tsao, Y. Hernandez, A. Hirsch, X. L. Feng and K. Müllen, *Adv. Mater.*, 2010, **22**, 5347–5377.
28 A. C. Ferrari, *Solid State Commun.*, 2007, **143**, 47–57.
29 Y. M. Shi, K. K. Kim, A. Reina, M. Hofmann, L. J. Li and J. Kong, *ACS Nano*, 2010, **4**, 2689–2694.
30 L. H. Zhang, Y. Jia, S. S. Wang, Z. Li, C. Y. Ji, J. Q. Wei, H. W. Zhu, K. L. Wang, D. H. Wu, E. Z. Shi, Y. Fang and A. Y. Cao, *Nano Lett.*, 2010, **10**, 3583–3589.
31 B. L. Sharma, in *Metal-Semiconductor Schottky Barrier Junctions and Their Applications*, Plenum Press, New York, 1984, Ch. 3.
32 S. M. Sze, in *Semiconductor Devices: Physics and Technology*, 2nd edn, John Wiley & Sons: New York, 2001.